



Published in final edited form as:

J Pharm Sci. 2018 December ; 107(12): 3153–3162. doi:10.1016/j.xphs.2018.07.032.

Three HIV Drugs, Atazanavir, Ritonavir, and Tenofovir, Coformulated in Drug-Combination Nanoparticles Exhibit Long-Acting and Lymphocyte-Targeting Properties in Nonhuman Primates

Simone Perazzolo¹, Laura M. Shireman¹, Josefin Koehn¹, Lisa A. McConnachie¹, John C. Kraft¹, Danny D. Shen¹, and Rodney J.Y. Ho^{1,2,*}

¹Department of Pharmaceutics, University of Washington, Seattle, Washington 98195

²Department of Bioengineering, University of Washington, Seattle, Washington 98195

Abstract

Drug-combination nanoparticles (DcNPs) administered subcutaneously represent a potential long-acting lymphatic-targeting treatment for HIV infection. The DcNP containing lopinavir (LPV)-ritonavir (RTV)-tenofovir (TFV), Targeted-Long-Acting-Antiretroviral-Therapy product candidate 101 (TLC-ART 101), has shown to provide long-acting lymphocyte-targeting performance in nonhuman primates. To extend the TLC-ART platform, we replaced TLC-ART 101 LPV with second-generation protease inhibitor, atazanavir (ATV). Pharmacokinetics of the ATV-RTV-TFV DcNP was assessed in macaques, in comparison to the equivalent free drug formulation and to the TLC-ART 101. After single subcutaneous administration of the DcNP formulation, ATV, RTV, and TFV concentrations were sustained in plasma for up to 14 days, and in peripheral blood mononuclear cells for 8 to 14 days, compared with 1 to 2 days in those macaques treated with free drug combination. By 1 week, lymph node mononuclear cells showed significant levels for all 3 drugs from DcNPs, whereas the free controls were undetectable. Compared with TLC-ART 101, the ATV-RTV-TFV DcNP exhibited similar lymphocyte-targeted long-acting features for all 3 drugs and similar pharmacokinetics for RTV and TFV, whereas some pharmacokinetic differences were observed for ATV versus LPV. The present study demonstrated the flexibility of the TLC-ART's DcNP platform to include different antiretroviral combinations that produce targeted long-acting effects on both plasma and cells.

Keywords

HIV; AIDS; long-acting; lipid nanoparticle(s) (LNP); drug-combination; preclinical pharmacokinetics; targeted therapy; targeted drug delivery

* Correspondence to: Rodney J.Y. Ho (Telephone: +1 206 543 3796). rodneyho@uw.edu (R.J.Y. Ho).

Introduction

Daily oral fixed-dose combination antiretroviral therapy is routinely used to suppress the plasma viral load of the HIV in patients. Combination antiretroviral therapy requires a high degree of patient adherence with likelihood of viral rebound if interrupted or discontinued. Rebounds may be due to residual HIV in cells of lymphoid tissues not adequately targeted by oral regime.¹ Since our initial proposal and discovery of low lymph tissue and cell drug exposure in patients after oral HIV drug therapy, the lymphoid tissue and cell drug insufficiency have been validated in prospective studies for multiple oral drug combination and fixed-dose combination therapy.² Thus, targeted long-acting strategies have been developed initially based on a single-drug nanosuspension³ and more recently using a novel, co-formulated drug-combination nanoparticle (DcNP) suspension approach,⁴ intended to target lymphocytes in tissues and blood.^{5,6} We previously published pharmacokinetic characterization of a novel DcNP formulation called Targeted-Long-Acting-Antiretroviral-Therapy product candidate 101 (TLC-ART 101), which combined 2 lipophilic protease inhibitors lopinavir (LPV) (log P = 5.9) and ritonavir (RTV) (log P = 6), plus 1 hydrophilic reverse transcriptase inhibitor tenofovir (TFV) (log P = -1.6), in a 4:1:3 molar ratio.⁴ Subcutaneously administered TLC-ART 101 has demonstrated to enhance localization of its 3 drugs—LPV, RTV, and TFV—together in the mononuclear cells of lymph nodes in nonhuman primates.⁴ After a single subcutaneous injection, TLC-ART 101 sustained significant drug concentrations in plasma and peripheral blood mononuclear cells (PBMCs) for up to 2 weeks. By contrast, when the same set of drugs were given subcutaneously in the free form, that is, not nanoformulated, plasma drug concentrations fell to near or below the limit of detection by 24 to 48 h. Moreover, TLC-ART 101 achieved efficient intracellular mononuclear cell concentrations when measured 1 week after administration, whereas the free-drug control was mostly undetectable.⁴

As combination HIV drug therapies evolve over time, especially with the introduction of newer and improved antiretroviral (ARV) drugs, there is a need to evaluate whether the TLC-ART nanoparticle platform is applicable across different combinations of ARVs. As the first step in a systematic investigation, we explored effects of substitution of the protease inhibitor by replacing LPV (log P = 5.9) in TLC-ART 101 with atazanavir (ATV), which is a widely deployed, second-generation protease inhibitor (log P = 4.5). ATV is highly selective for the HIV-1 protease with a reported 2- to 20-fold higher antiretroviral activity compared with several other commercialized protease inhibitors.⁷ In humans, oral ATV/RTV 300/100 mg once daily has demonstrated to be similar or higher antiviral activity compared with oral LPV/RTV 400/100 mg twice daily.⁸ Hence, a DcNP containing 2:1:3 molar ratio of ATV, RTV, and TFV, respectively, was prepared based on the same rigorous protocol, including in process controlled procedure, developed to produce for TLC-ART 101.⁹

In this report, we have characterized the effects of the DcNP on ATV-RTV-TFV long-acting pharmacokinetics in plasma and cells of nonhuman primates in comparison with those treated with equivalent free drug combination as a control. Noncompartmental and compartmental analyses (mechanism-based pharmacokinetic) were performed for the time-course plasma, PBMCs, and lymph node mononuclear cells (LNMCs) after a single subcutaneous administration in macaques. Parallel analyses were also performed to compare

the pharmacokinetics of the ATV-RTV-TFV DcNP with the TLC-ART 101 LPV-RTV-TFV formulation in macaques.

Materials and Methods

Materials and Animals

1,2-Distearoyl-sn-glycero-3-phosphocholine (DSPC) and 1,2-distearoyl-sn-glycero-3-phosphoethanolamine-N-[poly (ethylene glycol)2000] (DSPE-mPEG2000) (both GMP grade) were purchased from Genzyme Pharmaceuticals (>99% purity; Cambridge, MA). ATV (C38H52N6O7), RTV (C37H48N6O5S2), and TFV (C9H14N5O4P) were purchased from Waterstone Technology (>99% purity; Carmel, IN). Ficoll separation medium, Lymphoprep was purchased from Axis-Shield PoC AS (Oslo, Norway). 10X RBC lysis buffer was obtained from eBioscience Inc. (San Diego, CA). United States Pharmacopeia-grade dimethyl sulfoxide was obtained from Avantor Performance Materials (Center Valley, PA). Tween-20 was purchased from Roche Diagnostics GmbH (Mannheim, Germany). All injection vehicles were United States Pharmacopeia grade. Other reagents were of analytical grade or higher.

Pharmacokinetic study with the ATV-RTV-TFV DcNP was conducted in 4 adult male nonhuman primate macaques (*Macaca nemestrina*), weighing 5.5 ± 0.5 kg (mean \pm SD), under a protocol approved by the University of Washington Institutional Animal Care and Use Committee. Animals were housed and cared for by the Washington National Primate Research Center according to standard operating procedures.

Free-Drug Preparation

The free-drug suspension was prepared in the same molar ratio of 2:1:3 ATV:RTV:TFV as the DcNP formulation using injection-grade aqueous solutions and aseptic technique. ATV and RTV were dissolved to concentrations of 16 mg/mL and 8.2 mg/mL, respectively. Separately, a solution of 2% Tween-20 was prepared in water and sterilized by passage through a 0.2- μ m filter. The suspension and Tween-20 solutions were mixed 1:1 (v/v) to produce a suspension containing a final concentration of 8 mg/mL ATV and 4.1 mg/mL RTV. TFV was dissolved to 20 mg/mL in 0.5% sodium chloride with 60 mM sodium bicarbonate and given as a separate but concurrent injection.

DcNP Preparation

DcNPs composed of ATV, RTV, and TFV were prepared as described previously.⁹ Drugs were in a molar ratio of, ATV:RTV:TFV, 2:1:3. The molar ratio of total lipids relative to RTV was 38.3. Lipid excipients DSPC and DSPE-mPEG2000 at a molar ratio of 9:1 were used to stabilize the 3 drugs listed previously in aqueous suspension. Drugs and lipids were dissolved together in chloroform and ethanol (2:1 v/v) in a glass tube and then evaporated under controlled conditions with N₂ gas. Residual solvent was removed overnight under vacuum desiccation. The dried lipid-drug mixture was then rehydrated at 60°C for 2 h in 0.9% NaCl containing 20 mM sodium bicarbonate (pH 7.4).

For small-scale preparation of lipid nanoparticles, 200 μL samples were sonicated using a bath-type sonicator (Avanti Polar Lipids Inc., Alabaster, AL) until the sample was whitish nanosuspension. For the large-scale preparation, 45 mL hydrated lipid-drug mixtures were homogenized for 15 cycles with an Avestin EmulsiFlex-C5 (Avestin Inc., Ottawa, Ontario, Canada) operating at 5000-6000 psi. Osmolality of the final preparation was measured with a VAPRO 5520 vapor pressure osmometer (Wescor Inc., Logan, UT). Lipid-drug nanoparticles were stored at 4°C-8°C. Drug association efficiencies, as measured by equilibrium dialysis, were $99 \pm 8.2\%$, $92 \pm 7.1\%$, and $10 \pm 0.8\%$ for ATV, RTV, and TFV, respectively, as described previously⁹ (Table 1). The final DcNP formulations contained a well-characterized percentage of drug association for each drug. DcNPs had an average diameter of 6-62 nm.⁹ A scaled-up preparation of 45 mL was produced under aseptic conditions at pH 7.2-7.6 and osmolality 213.5 mOsm/kg, comparable with that of the laboratory-scale preparations of 0.2 mL.⁹

Pharmacokinetic Study of the ATV-RTV-TFV DcNP in Nonhuman Primates

Macaques were assigned to 2 treatment arms. The free-drug (control) arm consisted of 2 groups. In one group, 2 macaques were administered a single subcutaneous dose of 20 mg/kg ATV, 10.2 mg/kg RTV, and 12.3mg/kg TFV in combination dissolved in dimethyl sulfoxide and diluted with water to a volume of 20 mL. Free RTV and TFV displayed similar pharmacokinetics as those observed in the free-drug control group ($n = 3$) for the previous TLC-ART 101 study⁴ and therefore were pooled with the current control group ($n = 5$). The pharmacokinetic data for free RTV and free TFV formulations across the 2 studies were pooled to provide a sufficient number of monkeys for statistical comparisons with the pharmacokinetics of DcNP formulations. The pharmacokinetic data for animals treated with free RTV and TFV were similar, and therefore pooling data did not impact the overall time-course of these 2 drugs. In the DcNP arm, 2 macaques were administered a single 20-mL subcutaneous injection of lipid nanoparticles containing a combination of 25 mg/kg of ATV, 12.8 mg/kg of RTV, and 15.3 mg/kg of TFV ($n = 4$).

Venous blood samples were collected from a femoral vein at 0, 0.5, 1, 3, 5, 8, 24, 48, 120, 168, 192, and 336 h (14 days) after subcutaneous injection. Whole blood in ethylenediaminetetraacetic acid tubes was immediately centrifuged, and plasma was removed and frozen at -80°C until liquid chromatography with tandem mass spectrometry analysis.

Plasma drug concentrations were reported in unit of nanomolar. Noncompartmental parameters were estimated from plasma profiles for free and DcNP formulations using Phoenix WinNonlin (Certara, Princeton, NJ). The following noncompartmental parameters were estimated: area under the plasma concentration–time curve AUC extrapolated to infinity; terminal half-life ($t_{1/2}$); apparent clearance (CL/F); and mean body residence time (MBRT) based on moments extrapolated to infinity.

Intracellular concentrations of ATV, RTV, and TFV were initially calculated as picogram/million cells. For comparison to plasma extracellular drug concentrations, PBMC intracellular concentrations were converted to nanomolar based on an average mononuclear cell volume of 4×10^{-9} mL.¹⁰

Isolation of PBMCs and LNMCs

PBMCs were isolated from whole blood using density gradient centrifugation and divided into pellets of 2×10^6 cells each. Two axillary lymph nodes were surgically excised at 24 and 192 h after drug administration. LNMCs were isolated by pressing the tissue through a 100- μ m nylon cell strainer (Corning, Tewksbury, MA) into cell culture media, and cells, followed by similar treatment as that of PBMCs, were analyzed for drug concentrations based on 2×10^6 cells for each sample/timepoint. All samples were stored at -80°C before liquid chromatography with tandem mass spectrometry drug analysis.

Determination of Drug Levels in Plasma, PBMCs, and LNMCs

Plasma drug concentrations were measured using an assay developed and validated previously.¹¹ The lower limit of quantification was 0.01 nM for all 3 ARVs in plasma.

For determination of drug concentrations in PBMCs and LNMCs, pellets of 2×10^6 cells/tube were lysed using 200 μ L water/methanol (50:50 v/v). To ensure complete lysis, the samples were sonicated for 10 min. Subsequent extraction and analysis was the same as for plasma. The lower limit of quantification was 0.01 nM for lysed cell suspension concentration converted.

Compartmental Modeling

Compartmental modeling was carried out using SAAM II v2.3 (The Epsilon Group, Charlottesville, VA). A recently proposed mechanism-based pharmacokinetic (MBPK) model for subcutaneous administration of DcNPs was employed.¹² Briefly, the model featured uptake and sequestration of DcNPs by the lymphatics during first pass following its absorption from the injection site; subsequent release of DcNPs into the blood circulation occurred via 3 successive, time-delayed waves (Fig. 1). Liberation of free drug from the DcNPs is assumed to occur once the nanoparticles reaches the blood circulation. As a result, the systemic portion of the model comprised two submodels—one for DcNP and the other for free drug; sum of the concentrations in the two central (blood) compartments for the two submodels represented the measured plasma concentration. Based on drug-particle association data (Table 1), the model assumed that, at the subcutaneous site, ATV and RTV were 100% incorporated in the DcNP, whereas TFV was only 10% associated. The free, 90% fraction of the injected TFV dose was assumed to move directly into the vasculature from the subcutaneous space, skipping first pass through the lymphatics.

Statistics

Data and noncompartmental parameters were reported as geometric mean and 95% confidence interval when $n > 2$. Compartmental modeling parameter estimation was carried out using a weighted least-squares method according to an additive error model with 10% error (SAAM II v2; The Epsilon Group). For free ATV, where $n = 2$, the geometric mean subject was reported. For the rest of the data, the standard 2-stage approach was employed. Comparisons of the ATV-based DcNP with the previously published TLC-ART 101 were carried out using unpaired Student t-tests at 95% confidence level.

Differences in antiviral dosages between the free drug formulation and the DcNP formulation were due to loading into nanoparticles. Doses of free drug formulations were scaled to match the doses given in DcNP formulations, assuming dose linearity in this small dose variance.

Differences in antiviral dosages between ATV-RTV-TFV DcNP and LPV-RTV-TFV DcNP (TLC-ART-101) were accounted for comparison (ATV normalized by LPV), assuming that dosage differences fell within the linearity range.

Results

Effects of Subcutaneously Injected DcNPs on ATV, RTV, and TFV Drug Concentrations Time-Course in Plasma in Nonhuman Primates

To determine the effects of DcNPs on ATV, RTV, and TFV, we determined the time -course of each drug in both plasma and PBMCs over 336 h (2 weeks) for the macaques treated with either DcNP or the counterpart free soluble combination. The time-courses are presented in Figure 2. When the ATV-RTV-TFV DcNP was given as a single subcutaneous injection to the macaques, all 3 drugs showed sustained plasma concentrations up to 336 h (Figs. 2a-2c, solid lines), whereas when those macaques treated with the free 3 drugs, at equivalent dose, all free drugs fell below the limit of detection by 48 h (Figs. 2a-2c, dashed lines). The drugs' time-concentration profiles following a DcNP injection showed the long-acting characteristic and wave-like pattern as noted previously for TLC-ART 101 containing LPV, RTV, and TFV.¹²

We also analyzed the DcNP effects on cellular time-course of ATV, RTV, and TFV. When the ATV-RTV-TFV DcNP was given as a single subcutaneous injection to the macaques, sustained drug concentration in PBMCs up to 336 h for ATV and RTV, and up to 192 h for TFV, was observed (Figs. 2d-2f, solid lines), whereas when those macaques treated with the free 3 drugs, at equivalent dose, all free drugs fell below the limit of detection by 48 h from PBMC intracellular concentration (Figs. 2d and 2f, dashed lines), except for free RTV whose last PBMC concentration timepoint was detected at 48 h (Fig. 2e).

Noncompartmental Analysis of ATV-RTV-TFV DcNP and Free Formulation

Plasma time-courses were analyzed for pharmacokinetics characterization of ATV, RTV, and TFV either given in DcNP or as free form. Results from the noncompartmental analysis were presented in Tables 2 and 3. Compared with its soluble counterpart, DcNP-formulated ATV showed 5-fold higher plasma area under the curve (AUC, 3.2 vs. 0.6 h μ M), 4-fold lower CL/F (11 vs. 42 L/h/kg body weight), 110-fold longer apparent $t_{1/2}$ (469 vs. 4.3 h), and 116-fold longer MBRT (650 vs. 5.6 h). RTV in DcNP had similar AUC (4.4 vs. 3.3 h μ M) and CL/F (4 L/h/kg), with 17-fold longer $t_{1/2}$ (73 vs. 4.2 h) and 22-fold longer MBRT (110 vs. 11 h) compared with RTV delivered in free form. In contrast, remarkable DcNP effects in both exposure and persistence were observed for TFV. TFV delivered in DcNP had 35-fold higher AUC (3057 vs. 85 h μ M), 23-fold lower CL/F (0.004 vs. 0.46 L/h/kg), 7-fold higher $t_{1/2}$ (66 vs. 9.6 h), and 41-fold higher MBRT (103 vs. 2.5), compared with TFV in

free form. Hence, the incorporation of ATV and TFV in the nanoparticle formulation mainly led to persistent and higher plasma exposure per dose.

Effects of Subcutaneous DcNPs on ATV, RTV, and TFV on Intracellular Concentrations of Targeting Cells in Nonhuman Primates

Intracellular concentrations of PBMCs and LNMCs were measured as targeting metric of ARVs loaded in current DcNP. The data on cell targeting parameters are summarized in Tables 4 and 5. In comparing DcNP to free drug formulation, ATV achieved 33-fold higher intracellular PBMC drug levels measured by AUC_{PBMC} (435 vs. 13 h μM), along with 3-fold higher intracellular LNMC concentrations at 24 h (0.1 vs. 0.33 μM) and at 192 h (0.09 vs. 0.03 μM). We also evaluated drug uptake into the mononuclear lymphocyte populations *in vivo* by examining the cell-to-plasma concentration ratios, which are governed by cell-plasma drug transport and clearance, along with plasma clearance and intracellular processing. We also compared drug localization in LNMCs and PBMCs, the latter being readily accessible monocytes in blood and could serve as a biomarker for lymph node monocyte population. When ATV from DcNP formulation is compared with free ATV, LNMC-to-plasma ratio was 4-fold lower at 24 h (13 vs. 57) and LNMC-to-PBMC ratio was 37-fold lower at 24 h (0.7 vs. 11); these lower ratios largely reflect the fact that plasma and PBMC concentrations were sustained after DcNP injection compared with after free drug injection. Animals treated with RTV in DcNP formulation exhibited 1.5-fold higher AUC_{PBMC} (79 vs. 22 h μM), 3-fold higher LNMC concentration at 24 h (0.40 vs. 0.14 μM), 13-fold higher LNMC-to-plasma ratio at 24 h (21 vs. 1.6), and similar LNMC-to-PBMC at 24 h (1 vs. 0.76) compared with RTV in free form. TFV in DcNP had 5-fold higher AUC_{PBMC} (1134 vs. 260 h μM) compared with TFV in free form. In the DcNP study, the LNMC sample for TFV at 24 h was missing. Also, free drugs were consistently undetectable at 192 h in all the macaques; therefore, free drug ratios were not available for this late timepoint.

Comparison of Current DcNP Containing ATV, RTV, and TFV with the Reported TLC-ART 101 Containing LPV, RTV, and TFV

Previously, we reported successful development of long-acting and lymphocyte-targeted 3-drug combination DcNP, called TLC-ART 101 formulation containing LPV, RTV, and TFV⁴; the current DcNP contained both RTV and TFV, but LPV was replaced with ATV. Thus, we have evaluated the pharmacokinetic parameters as a comparison with the current DcNP with that of TLC-ART 101. Time-courses, plasma noncompartmental analysis and cell-targeting values of TLC-ART 101 were reported in Figure 3 and Tables 4-6, respectively.

Figure 3 compares drug concentration-time profiles in plasma and PBMCs between ATV-RTV-TFV in DcNP and LPV-RTV-TFV in TLC-ART 101. RTV and TFV exhibit similar plasma and PBMC profiles (Fig. 3), whereas plasma concentration of ATV was 2 orders of magnitudes lower than that of LPV at equivalent dose over the entire 14-day study period (Fig. 3a). Noncompartmental analysis yielded significantly smaller AUC of ATV compared with LPV (3.2 vs. 11 h μM , $p < 0.01$, Table 2). A corresponding difference in CL/F was observed (11 vs. 0.85 L/h/kg, $p < 0.01$, Table 2). ATV in DcNP also had significantly higher

AUC_{PBMC} than LPV in DcNP (435 vs. 79 h μ M, $p < 0.01$, Table 4). RTV in the ATV-RTV-TFV DcNP showed a statistically significantly lower LNMC concentration and LNMC-to-PBMC ratio than for RTV in TLC-ART 101 (0.4 vs. 6.3 mM and 1.0 vs. 8.9, $p = 0.01$, Table 4).

Comparisons between free ATV and free LPV had lower plasma AUC (0.6 vs. 4.8 h μ M) and higher CL/F (42 vs. 5 L/h/kg), as observed for the same drugs but in DcNP form, although no statistical test could be done due to $n = 2$ for free ATV (Table 3). This could indicate that DcNP pharmacokinetic differences between ATV and LPV observed may have stemmed from free drug pharmacokinetics. Comparison of PBMC and LNMC data between free ATV and free LPV was possible only for AUC_{PBMC} as LPV LNMC concentrations were undetectable at 24 h and 192 h⁴; AUC_{PBMC} between free ATV and free LPV did not show significant difference.

Compartmental Modeling Results

These data were analyzed further following a MBPK model previously developed and validated with TLC-ART 101 subcutaneous dosing of DcNP containing LPV, RTV, and TFV. Based on the MBPK model schematically depicted in Figure 1, the experimental data are fitted for each drug—ATV, RTV, and TFV—formulated as a combination DcNP and graphically presented in Figure 4. We found that time-course kinetics of each drug in DcNP within TLC-ART 101 fit well with R^2 of 0.94, 0.90, and 0.96 for ATV, RTV, and TFV, respectively (Fig. 4). The fitting generated a set of parameters reported in Table 6, which may be useful to enhance the pharmacokinetics interpretation of DcNP drugs given subcutaneously. First-pass parameters k_{12} , k_{31} , k_{41} and $tlag_1$, $tlag_2$, $tlag_3$ represented the rates and delays of the 3 lymphatic pathways and gave rise to the peculiar plasma undulations. TFV was thus quicker to enter circulations while ATV and RTV lymphatic first pass were comparably slower. This is in accordance with the fact that the hydrophilic compound TFV has association efficiency lower compared with the other lipophilic drugs in the combination (Table 1). Although free drug plasma apparent volume of distribution pool (V_{7_free}) was similar between ATV and RTV (but greatly lower for TFV), the apparent volume of distribution of the DcNP-associated drug plasma pool (V_{5_DcNP}) was greatly higher for ATV compared with the rest of the drugs. This, combined to the slower release parameter k_{75} , might indicate that ATV could be greatly associated with DcNP *in vivo*, although experimental confirmation is needed.

Comparison of model parameter estimates between ATV-RTV-TFV DcNP and LPV-RTV-TFV TLC-ART 101¹² revealed significant differences between ATV and LPV for V_{5_DcNP} and k_{75} ($p < 0.01$, Table 6). V_{5_DcNP} was 180-fold higher for ATV than LPV (1259 vs. 7 L/kg). k_{75} was the rate constant for release of free drug from DcNP in plasma; this estimate was 18-fold lower for ATV than LPV (0.04 vs. 0.7 1/h). Both observations are consistent with the very low but sustained circulating level of ATV compared with LPV when they are administered in DcNP formulations. Comparison across DcNP formulations did not report differences in MBPK parameters between RTV and TFV (Table 6).

Taken together, these data indicate that ATV, RTV, and TFV in DcNP—based on the TLC-ART platform—provided sustained plasma and PBMC intracellular concentrations for 2

weeks of study in macaques. A greatly improved lymphocyte targeting is achieved with drug combination coformulated in DcNP both in blood periphery (PBMCs) and lymph nodes (LNMCs) in macaques. Compared with previously reported DcNP with LPV, RTV, and TFV, called TLC-ART 101,⁴ current DcNP with ATV replacing LPV had similar targeted long-acting features found in TLC-ART 101, where intracellular ATV exposure may be higher than that of LPV.

Discussion

Taking advantage of the ability to co-formulate ATV, RTV, and TFV in a stable and scalable drug-combination nanosuspension (DcNP) for nonhuman primate studies, we have evaluated the effects of DcNPs on pharmacokinetics with respect to long-acting plasma drug levels and targeted lymphocyte accumulation in macaques. We found that nanoparticles formulated with a combination of 3 HIV drugs, ATV-RTV-TFV, exhibited sustained plasma levels for the 2-week study and intracellular levels persisting at higher than plasma drug levels. Compared with free drug combination, subcutaneous injection in nonhuman primates of the same set of drugs (ATV, RTV, and TFV) in this DcNP formulation exhibited sustained plasma, PBMC, and LNMC drug concentrations for the 2-week study; as opposed to within few days in primates receiving equivalent free drug combination.

This study is a follow-on investigation to a recently published study on the original DcNP preparation, called TLC-ART 101 containing LPV, RTV, and TFV.⁴ The current report replaces LPV in the TLC-ART 101 drug combination with another hydrophobic HIV protease inhibitor ATV. ATV is a widely used protease inhibitor used in HIV treatments and often deployed as a replacement of LPV. Pharmacokinetics of RTV and TFV in macaques for current ATV-RTV-TFV DcNP formulation was consistent with those observed for TLC-ART 101.⁴ However, there are some differences in the protease inhibitor ATV and LPV distribution and pharmacokinetic profiles, although both exhibit long-acting cell and plasma behavior over the 2-week study in macaques.

ATV has been previously nanoformulated,⁹ for example, to increase ATV brain barrier penetration,¹³ or in combination with RTV for HIV long-acting therapy.¹⁴ Thus, at 24 and 192 h after dosing as an ATV-RTV-TFV DcNP subcutaneous injection in primates, ATV and TFV intracellular concentrations of peripheral blood mononuclear cells in primates exhibit levels that exceed effective concentrations to suppress HIV. ATV in LNMCs was 100 nM and 90 nM at 24 and 192 h after injection, respectively (Table 4), which are greater than reported *in vitro* effective concentration that produces 90% of the maximal effect (EC_{90}) = 13 nM.¹⁵ Similarly, TFV in LNMCs was 130 nM at 192 h after injection (Table 4), which is greater than *in vivo* EC_{50} = 49 nM in nonhuman primates.² In particular, TFV is a hydrophilic compound quickly cleared from circulation when given in free form; however, when presented in such DcNPs, plasma and PBMC exposure greatly improved. Overall, the ATV-RTV-TFV DcNP provided extended PBMC and LNMC effective drug concentrations, far exceeding those achieved with free drug combination treatment.

Pharmacokinetic comparison of the current ATV-based DcNP and LPV-based (TLC-ART 101⁴) formulation revealed 2 key findings: (1) pharmacokinetics of the hydrophilic TFV was

not altered by the exchange of hydrophobic protease inhibitors and (2) pharmacokinetics of the protease inhibitor booster RTV was largely unaltered by the exchange of hydrophobic protease inhibitors. These observations suggest that the pharmacokinetics of the constituent drugs is not influenced by the co-formulated drugs; that is, they may maintain independent pharmacokinetics with no apparent evidence of biophysical interaction between drug components within the DcNP. Further *in vitro* and *in vivo* studies are needed to substantiate this preliminary finding. Nonetheless, we found a lower trend in RTV concentration in LNMCs at 24 h, along with a reduced LNMC-PBMC ratio, when LPV was replaced by ATV. Although this unexpected finding may suggest some subtle interactions between the 2 protease inhibitors within the DcNP, caution is warranted in drawing a definitive conclusion as the molar ratio of lipid-to-drug and that of drug components, while similar, were not identical between the 2 nanoformulations (Table 1). Although possible, clinical significance of an alteration in RTV uptake into LNMCs is known, RTV is not considered an active drug in the both TLC-ART 101 and ATV containing DcNP formulations; it was included because of its standard use as a booster in all current oral protease inhibitor regimens.¹⁶ Whether RTV acts as a booster for subcutaneous dosage form of protease inhibitors is an open question. Thus, the observed differences for RTV for LNMC targeting may not impact the anti-HIV potency of the LPV or TFV within drug combinations employed in respective DcNP formulation.

ATV in the present DcNP formulation exhibited a lower plasma exposure (or higher apparent clearance) than LPV in TLC-ART 101 (Table 2). This may be explained to some extent by inherent differences in the pharmacokinetics of these 2 protease inhibitors in free form. In macaques, free ATV had a 9-fold higher CL/F or 8-fold lower AUC compared with free LPV (Table 3). Furthermore, previous intravenous pharmacokinetics study of free ATV in humans showed 2 orders of magnitude lower plasma concentrations compared with the same dose of free LPV.¹⁷ ATV exhibited a 5.5-fold higher PBMC exposure than LPV (AUC_{PBMC}, Table 4); hence, the 2 protease inhibitors may have similar targeting capabilities. Preclinical study in an appropriate HIV infection model may help to determine whether this apparent PBMC-targeting difference is meaningful. Other explanations, such as differences in the release rate of free ATV versus free LPV from DcNPs, cannot be ruled out. In fact, modeling parameter k_{75} —release rate of free drug from DcNPs—suggests that ATV is predicted to exhibit lower rate of dissociation from DcNPs than that for LPV (Table 6). However, *in vivo* nanoparticles dissociation from DcNPs is difficult to measure directly and it is a complex multifactorial process.¹⁸

The long-acting mechanisms of subcutaneous HIV drug combination formulated in DcNP has yet to be fully elucidated. Current working hypothesis is that after subcutaneous dosing, drugs associated to DcNP are readily cleared from injection site, and preferentially taken up collectively into lymph as a first pass where there may be an extensive distribution to both central and peripheral lymph nodes. Nanoparticles could be retained in the sinuses of lymph nodes or accumulate in lymphoid tissues. They could be gradually taken up by mononuclear cells that transit in and out the node and peripheral blood. The nanoparticles taken up by mononuclear cells in the lymph and blood may contribute to the slow release of DcNP-bound drugs into circulation. Looking at the reported DcNP ATV terminal half-life of around 20 days (Table 2), plasma concentrations may linger efficiently for more than 2

weeks. The model, based on the experimental data in macaques, revealed that lymphatic release occurs in 3 stages or waves: fast (t_{lag1}), moderate (t_{lag2}), and slow (t_{lag3}) transit through the lymphatic network (Table 6). This model has been described in greater details in our previous publication for TLC-ART 101.¹² Each wave of release generates a lagged plasma peak that may explain the peculiar undulating pharmacokinetics of drugs loaded in DcNP. The observed statistical differences between ATV and LPV in model parameters reflect the pharmacokinetic differences discussed previously. Although such mechanism-based models have great flexibility in representing the pharmacokinetics of DcNP drugs, a physiological-based pharmacokinetic modeling approach, featuring a whole-body lymphatic network, may be beneficial to gain further insights on absorption, distribution, and targeting of DcNPs.^{19,20}

Through data collected in the present study, we found that the TLC-ART platform can be optimized to accommodate a different ARV combination, at least for an alteration in the protease inhibitor component, and still achieve the necessary targeted and long-acting features. Although replacing LPV with ATV may not represent a clear pharmacological advantage, other hydrophobic and perhaps hydrophilic HIV drugs could yield a more potent targeted, long-acting delivery system. For example, studies are currently underway in our laboratory to investigate whether tenofovir disoproxil fumarate, tenofovir alafenamide, or emtricitabine could be exchanged for TFV. The TLC-ART platform has recently been extended to include coformulations of 4 drugs adding in another nucleoside reverse transcriptase inhibitor lamivudine (LPV, RTV, TFV, and 3TC).²¹ Feasibility of these extended approaches will depend on association efficiency of the component ARVs to the nanoparticles; for instance, the protease inhibitor darunavir was found to be unstable in lipid nanoparticles.⁹ Given the potential flexibility of the DcNP platform, it could be applied to drug targeting of hepatitis B,⁵ tuberculosis,²² or tumors.²³

In summary, using protease inhibitors for HIV treatment ATV, combined with RTV and TFV into a DcNP, based on the TLC-ART platform, resulted in lymphocyte-targeted, long-acting pharmacokinetics of all 3 HIV drugs in nonhuman primates. ATV, a newer protease inhibitor, could replace LPV in TLC-ART 101 DcNP nanoformulation for consideration long-acting product development. We demonstrated that the TLC-ART platform may have the flexibility to accommodate diverse ARV combinations for development of long-acting and targeted therapy for HIV/AIDS and other diseases.

Acknowledgments

This study was supported by NIH grant UM1 AI120176, and in part by P51 OD010425, and AI 077390.

The authors wish to express their appreciation to Jinghua Duan and Jennifer Freeling for their input on ATV containing DcNP formulations and the Washington National Primate Center Research Support Group for their support of the NHP studies.

References

1. Fletcher CV, Staskus K, Wietgreffe SW, et al. Persistent HIV-1 replication is associated with lower antiretroviral drug concentrations in lymphatic tissues. *Proc Natl Acad Sci U S A*. 2014;111(6):2307–2312. [PubMed: 24469825]

2. Freeling JP, Ho RJ. Anti-HIV drug particles may overcome lymphatic drug insufficiency and associated HIV persistence. *Proc Natl Acad Sci U S A*. 2014;111(25):E2512–E2513. [PubMed: 24889644]
3. McMillan J, Szlachetka A, Slack L, et al. Pharmacokinetics of a long-acting nanoformulated dolutegravir prodrug in rhesus macaques. *Antimicrob Agents Chemother*. 2018;62(1):e01316–e01317. [PubMed: 29061742]
4. Kraft JC, McConnachie LA, Koehn J, et al. Long-acting combination anti-HIV drug suspension enhances and sustains higher drug levels in lymph node cells than in blood cells and plasma. *AIDS*. 2017;31(6):765–770. [PubMed: 28099191]
5. Kraft JC, Freeling JP, Wang Z, Ho RJ. Emerging research and clinical development trends of liposome and lipid nanoparticle drug delivery systems. *J Pharm Sci*. 2014;103(1):29–52. [PubMed: 24338748]
6. Müller RH, MaÈder K, Gohla S. Solid lipid nanoparticles (SLN) for controlled drug delivery—a review of the state of the art. *Eur J Pharm Biopharm*. 2000;50(1):161–177. [PubMed: 10840199]
7. Sparidans RW, Dost F, Crommentuyn KM, Huitema AD, Schellens JH, Beijnen JH. Liquid chromatographic assay for the protease inhibitor atazanavir in plasma. *Biomed Chromatogr*. 2006;20(1):72–76. [PubMed: 15954163]
8. Molina J-M, Andrade-Villanueva J, Echevarria J, et al. Once-daily atazanavir/ritonavir versus twice-daily lopinavir/ritonavir, each in combination with tenofovir and emtricitabine, for management of antiretroviral-naïve HIV-1-infected patients: 48 week efficacy and safety results of the CASTLE study. *Lancet*. 2008;372(9639):646–655. [PubMed: 18722869]
9. Duan J, Freeling JP, Koehn J, Shu C, Ho RJ. Evaluation of atazanavir and darunavir interactions with lipids for developing pH-responsive anti-HIV drug combination nanoparticles. *J Pharm Sci*. 2014;103(8):2520–2529. [PubMed: 24948204]
10. Simiele M, D'Avolio A, Baietto L, et al. Evaluation of the mean corpuscular volume of peripheral blood mononuclear cells of HIV patients by a coulter counter to determine intracellular drug concentrations. *Antimicrob Agents Chemother*. 2011;55(6):2976–2978. [PubMed: 21402849]
11. Koehn J, Ding Y, Freeling J, Duan J, Ho RJ. A simple, efficient, and sensitive method for simultaneous detection of anti-HIV drugs atazanavir, ritonavir, and tenofovir by use of liquid chromatography-tandem mass spectrometry. *Antimicrob Agents Chemother*. 2015;59(11):6682–6688. [PubMed: 26248367]
12. Kraft JC, McConnachie LA, Koehn J, et al. Mechanism-based pharmacokinetic (MBPK) models describe the complex plasma kinetics of three antiretrovirals delivered by a long-acting anti-HIV drug combination nanoparticle formulation. *J Control Release*. 2018;275:229–241. [PubMed: 29432823]
13. Chattopadhyay N, Zastre J, Wong H-L, Wu XY, Bendayan R. Solid lipid nanoparticles enhance the delivery of the HIV protease inhibitor, atazanavir, by a human brain endothelial cell line. *Pharm Res*. 2008;25(10):2262–2271. [PubMed: 18516666]
14. Gautam N, Roy U, Balkundi S, et al. Preclinical pharmacokinetics and tissue distribution of long-acting nanoformulated antiretroviral therapy. *Antimicrob Agents Chemother*. 2013;57(7):3110–3120. [PubMed: 23612193]
15. Robinson BS, Riccardi KA, Gong YF, et al. BMS-232632, a highly potent human immunodeficiency virus protease inhibitor that can be used in combination with other available antiretroviral agents. *Antimicrob Agents Chemother*. 2000;44(8):2093–2099. [PubMed: 10898681]
16. Kumar GN, Dykstra J, Roberts EM, et al. Potent inhibition of the cytochrome P-450 3A-mediated human liver microsomal metabolism of a novel HIV protease inhibitor by ritonavir: a positive drug-drug interaction. *Drug Metab Dispos*. 1999;27(8):902–908. [PubMed: 10421617]
17. Noor MA, Parker RA, O'mara E, et al. The effects of HIV protease inhibitors atazanavir and lopinavir/ritonavir on insulin sensitivity in HIV-seronegative healthy adults. *AIDS*. 2004;18(16):2137–2144. [PubMed: 15577646]
18. Bertrand N, Leroux JC. The journey of a drug-carrier in the body: an anatomo-physiological perspective. *J Control Release*. 2012;161(2):152–163. [PubMed: 22001607]

19. Rajoli RK, Back DJ, Rannard S, et al. Physiologically based pharmacokinetic modelling to inform development of intramuscular long-acting nanoformulations for HIV. *Clin Pharmacokinet.* 2015;54(6):639–650. [PubMed: 25523214]
20. Siccardi M, Owen A. Towards a computational prediction of nanoparticle pharmacokinetics and distribution. *J In Silico In Vitro Pharmacol.* 2016; 2(1):1–8.
21. McConnachie LA, Kinman LM, Koehn J, et al. Long-acting profile of 4 drugs in 1 anti-HIV nanosuspension in nonhuman primates for 5 weeks after a single subcutaneous injection. *J Pharm Sci.* 2018;30:1–4.
22. Swindells S, Siccardi M, Barrett S, et al. Long-acting formulations for the treatment of latent tuberculous infection: opportunities and challenges. *Int J Tuberc Lung Dis.* 2018;22(2):125–132. [PubMed: 29506608]
23. Wong HL, Bendayan R, Rauth AM, Li Y, Wu XY. Chemotherapy with anticancer drugs encapsulated in solid lipid nanoparticles. *Adv Drug Deliv Rev.* 2007;59(6): 491–504. [PubMed: 17532091]

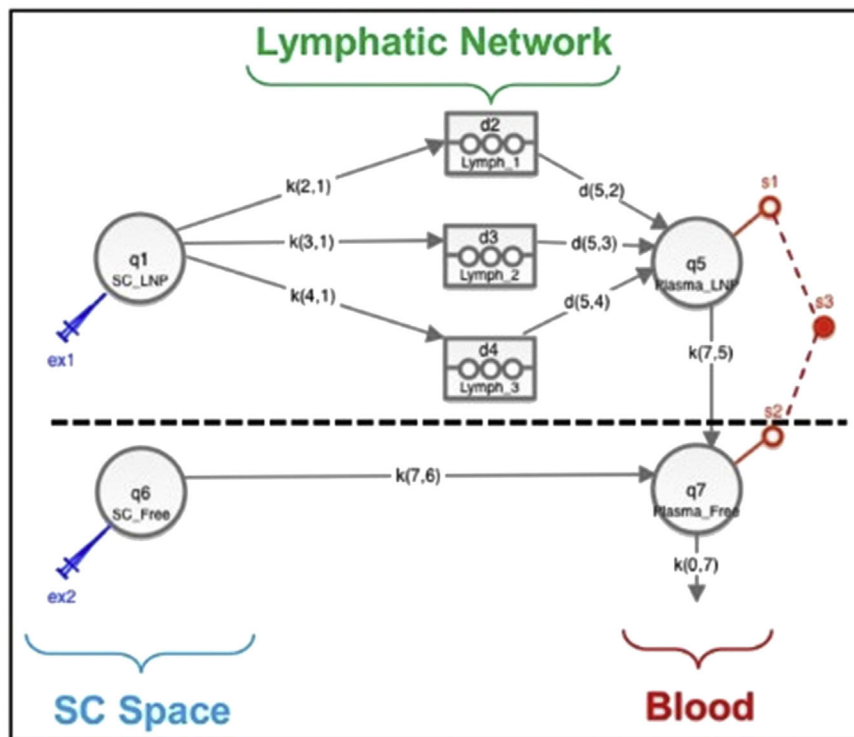


Figure 1. MBPK model schematics for the pharmacokinetics of DcNP subcutaneously administered. The model has been thoroughly presented elsewhere.¹² Briefly, the model features 2 portions, one for the DcNP uptake (above dashed line) and one for the free drug uptake (below dashed line). Above dashed line: Uptake of DcNPs from injection site (q1 – SC_LNP) to the lymphatics (k21, k31, k41) and subsequent release into the blood circulation (d52, d53, d54) was modeled by 3 successive, time-delayed compartments (d2 – Lymph_1, d3 – Lymph_2, d4 – Lymph_3). Liberation of free drug from DcNP (k75) was assumed to occur once the nanoparticles reaches the blood circulation (q5 – Plasma_LNP). Below dashed line: Uptake of free drugs from injection site (q6 – SC_Free) to blood circulation (q7 – Plasma_Free) was modeled by a free drug uptake rate (k76). To q7 – Plasma_Free connects q5 – Plasma_LNP. Plasma concentration measurements (s3) were the sum of systemic q7 – Plasma_Free and q5 – Plasma_LNP concentrations (s1, s2), being plasma concentrations of DcNP and equivalent free form measured indistinguishably. Parameters K represented linear kinetics rates. Based on drug-particle association data, the model assumed that, at the subcutaneous site, ATV and RTV were 100% incorporated in the DcNP, whereas TFV was only 10% associated (above dashed line), whereas the 90% fraction of the injected TFV dose was assumed to be free (below dashed line).

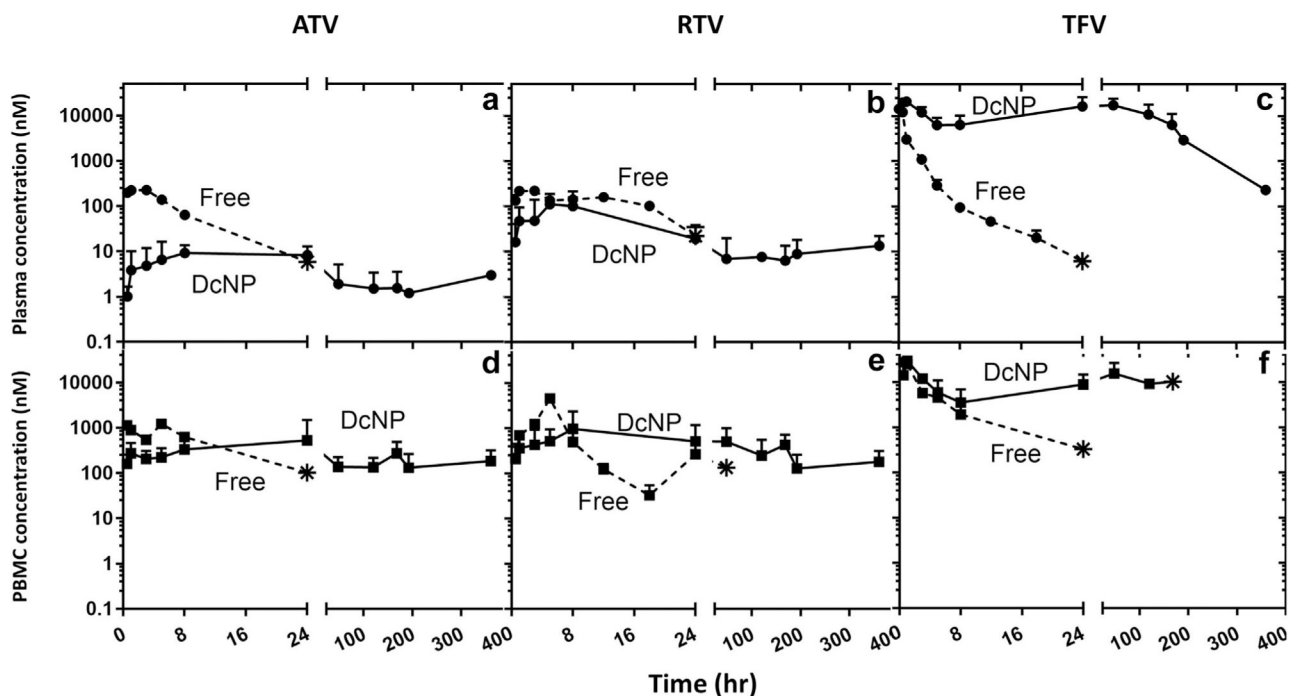


Figure 2.

Effects of DcNP formulation ATV, RTV, and TFV on plasma and blood mononuclear cells in nonhuman primates. A single subcutaneous dose of ATV, RTV, and TFV drug was administered as nanocombination (DcNP) or as free drug equivalent. The 3 drug concentrations in plasma and PBMCs were monitored over 14 d (336 h). Upper panels (a-c) describe plasma concentration comparison of DcNP (solid lines) and free drugs (dashed lines). Lower panels (d-f) describe time-course of PBMC concentration comparison of DcNP (solid lines) and free drugs (dashed lines). Free drugs were scaled to dosages equivalent to those in DcNP. Circle symbols are plasma timepoints. Square symbols are PBMC timepoints. Star symbols represent the last detectable timepoint. Limit of detection 0.01-0.03 pmol/mL. No data points were plotted for measured drug levels that fell below the limit of detection. Data expressed were geometric mean (\pm SD).

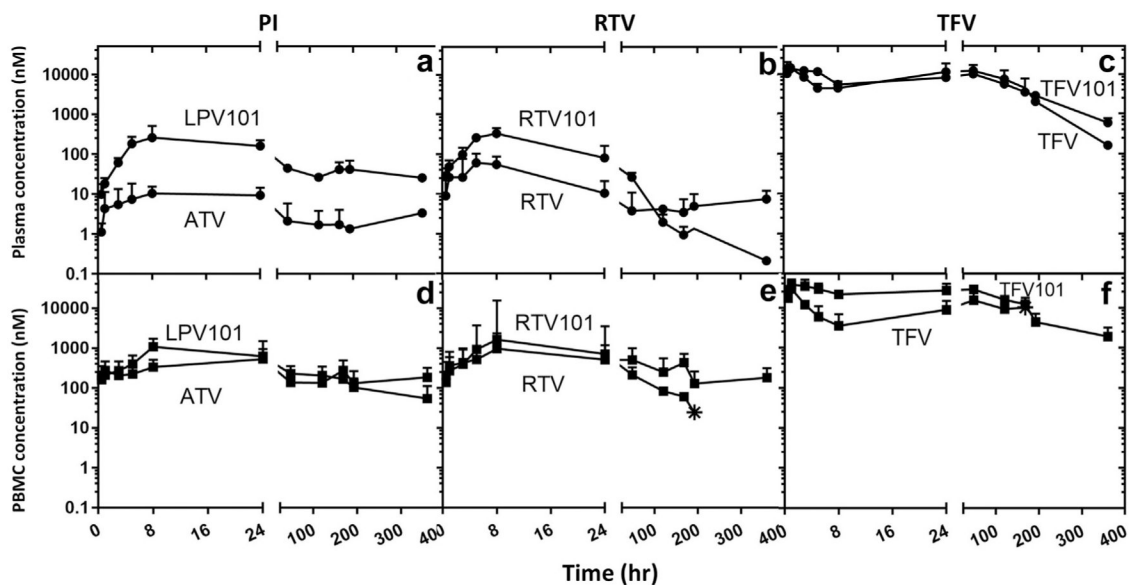


Figure 3.

Effects on plasma and blood mononuclear cells in nonhuman primates when substituting protease inhibitors, ATV in place of LPV. A single subcutaneous dose of ATV, RTV, and TFV drug was administered as nanocombination (DcNP) and compared with previously reported TLC-ART 101 LPV, RTV, and TFV.⁴ The 3 drug concentrations in plasma and PBMCs were monitored over 14 d (336 h). TLC-ART 101 drug plots are appended with “101” to distinguish them from current DcNP drugs. Upper panels (a-c) describe plasma concentration comparison of current ATV-RTV-TFV DcNP and previously reported TLC-ART 101 LPV-RTV-TFV. Lower panels (d-f) describe time-course of PBMC concentration comparison of current ATV-RTV-TFV DcNP and previously reported TLC-ART 101 LPV-RTV-TFV. Current ATV-RTV-TFV DcNP dosages were scaled to dosages equivalent to those in TLC-ART 101. Circle symbols are plasma timepoints. Square symbols are PBMC time-points. Star symbols represent the last detectable timepoint. Limit of detection 0.01-0.03 pmol/mL. No data points were plotted for measured drug levels that fell below the limit of detection. Data expressed were geometric mean (\pm SD).

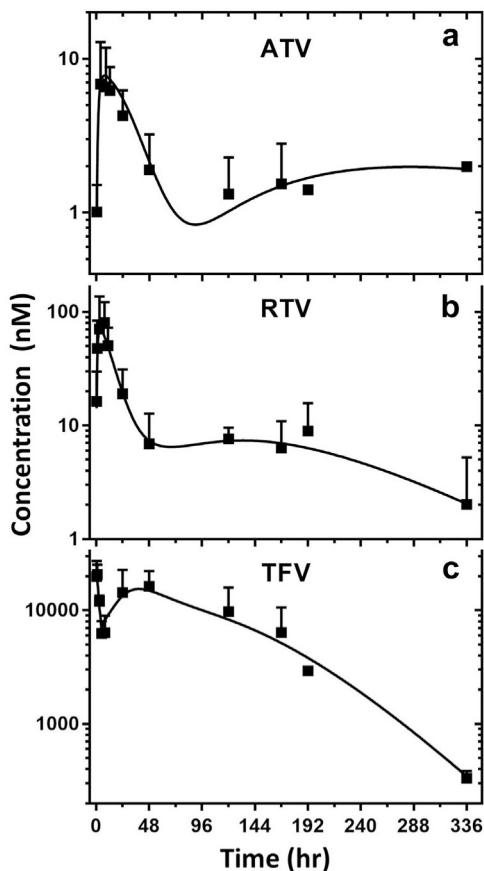


Figure 4.

The plasma time-course of experimental and fitted data for TLC-ART 101 based on the MBPK model. MBPK-predicted and experimental average plasma concentration-time profiles for ATV (panel A), RTV (panel B), and TFV (panel C) are presented. The regression analysis of the fitted time-course drug concentration provides R^2 of 0.94, 0.90, and 0.96 for ATV, RTV, and TFV, respectively. The model parameter estimates are presented in Table 6. Model prediction is displayed as solid lines and observed DcNP data as squares (geometric mean \pm CV), for panel a: DcNP ATV, panel b: DcNP RTV, and panel c: DcNP TFV.

Table 1

Characterization of Current ATV-RTV-TFV DcNP and Previously Published TLC-ART 101

Formulation	Protease Inhibitors		Reverse Transcriptase
	ATV	RTV	TFV (PMPA)
ATV-RTV-TFV ^a	ATV	RTV	TFV (PMPA)
Molar ratio relative to RTV	2	1	3
% Association to DcNP	99 ± 8	92 ± 7	10 ± 1
TLC-ART 101 ^b	Lopinavir	RTV	TFV (PMPA)
Molar ratio relative to RTV	4	1	5
% Association to DcNP	92 ± 6	91 ± 7	10 ± 3

PMPA, 9-(2-Phosphonyl-methoxypropyl)adenine.

^aATV-RTV-TFV DcNP was prepared accordingly to TLC-ART platform with DSPC-DSPE-mPEG2000 (9:1).⁹^bFrom previous study.⁴

Table 2
 Plasma DcNP Noncompartmental Pharmacokinetics Parameters Comparison of Current ATV-RTV-TFV and Previously Reported TLC-ART 101 Containing LPV-RTV-TFV

Parameter	DcNP Containing ATV			DcNP Containing LPV (TLC-ART 101)		
	ATV	RTV	TFV	LPV	RTV	TFV
AUC (h·µM)	3.2 ^a (1.5-4.4)	4.4 (1.4-14.0)	3057 (1029-9078)	11 ^a (8.0-13)	4.8 (2.2-7.9)	416 (320-470)
CL/F (L/(h·kg))	11 ^a (8-13)	4 (2-13)	0.004 (0.002-0.015)	0.85 ^a (0.11-1.80)	1.4 (0.8-2.1)	0.020 (0.012-0.027)
Terminal t _{1/2} (h)	469 (330-654)	73 (36-175)	66 (29-185)	476 (232-1010)	44 (20-66)	65 (58-75)
MBRT (h)	650 (370-1230)	110 (46-266)	128 (65-254)	116 (39-328)	25 (22-27)	103 (99-108)

Geometric Mean (95% CI).

Free drugs scaled to equivalent DcNP dosages. DcNP containing ATV drugs scaled to equivalent DcNP containing LPV (TLC-ART 101)⁴ drug dosages.

DcNP containing LPV (TLC-ART 101) drugs and free LPV values were taken from previous TLC-ART 101 study.⁴

AUC, area under the plasma drug concentration-time curve extrapolated to infinity; t_{1/2}, apparent terminal plasma drug half-life; CL/F, apparent total clearance; MBRT, mean body residence time extrapolated to infinity; – not detected; NA, not available.

^aUnpaired t-test $p < 0.05$ between formulations.

Table 3

Plasma Free Drug Noncompartmental Pharmacokinetics Parameters Comparison of Current ATV, RTV, and TFV and Previously Reported Free LPV

Free Drugs	ATV	RTV ^a	TFV ^a	LPV
AUC (h·µM)	0.6 ^b	3.3 (2.6-3.9) ^d	85 (72-93) ^d	4.8 (4.2-4.6) ^c
CL/F (L/(h·kg))	42 ^b	4.0 (2.3-5.7) ^d	0.46 (0.31-0.93) ^d	4.6 (4.1-5.3) ^c
Terminal t _{1/2} (h)	4.3 ^b	4.2 (3.3-5.9) ^d	9.6 (1.4-11.3) ^d	8.7 (5.3-10.4) ^c
MBRT (h)	5.6 ^b	10.5 (7.6-13.2) ^d	2.5 (1.6-3.5) ^d	11.0 (10.6-11.4) ^c

Geometric Mean (95% CI).

Free drugs scaled to equivalent DeNP dosages. DeNP containing ATV drugs scaled to equivalent DeNP containing LPV (TLC-ART 101⁴) drug dosages.

DeNP containing LPV (TLC-ART 101) drugs and free LPV values were taken from previous TLC-ART 101 study.⁴

AUC, area under the plasma drug concentration-time curve extrapolated to infinity; t_{1/2}, apparent terminal plasma drug half-life; CL/F, apparent total clearance; MBRT, mean body residence time extrapolated to infinity; – not detected; NA, not available.

^aRTV and TFV merged with previous free drugs results.⁴

^bn = 2.

^cn = 3.

^dn = 5.

Table 4
Target Mononuclear Cell Values of Drugs From DeNP for Current ATV-RTV-TFV DeNP and Previously Reported TLC-ART 101 Containing LPV, RTV, and TFV

Parameter	DeNP Containing ATV			DeNP Containing LPV (TLC-ART 101)		
	ATV	RTV	TFV	LPV	RTV	TFV
AUC _{PBMC} (h·µM)	435 ^a (302-580)	85 (9-150)	1134 (588-1554)	79 ^a (33-120)	52 (16-92)	435 (166-987)
LNMC						
24 h (µM)	0.10 (0.04-0.24)	0.40 ^a (0.06-3.00)	NA	14 (6-40)	6.3 ^a (4.4-8.5)	25 (14-47)
192 h (µM)	0.09 ^b	0.35 ^b	0.13 ^b	5 0.0 (0.4-13.1)	1.00 (0.06-2.00)	19 (3.6-280)
LNMC/plasma						
24 h	13 (6-25)	21.2 (9.5-75.0)	NA	90 (13-700)	78 (18-280)	3 (1.5-5.3)
192 h	69	23 ^b	80 ^b	198 (128-560)	-	6.8 (1.4-75)
LNMC/PBMC						
24 h	0.7 (0.02-5.02)	1.0 ^a (0.3-3.8)	-	23 (8-170)	8.9 ^a (3.9-13.0)	0.93 (0.39-2.3)
192 h	2.4 ^b	0.7 ^b	-	79 (51-170)	-	4.4 (0.45-340.0)

Geometric Mean (95% CI).

Free drugs scaled to equivalent DeNP dosages. DeNP containing ATV drugs scaled to equivalent DeNP containing LPV (TLC-ART 101)⁴ drug dosages. DeNP containing LPV (TLC-ART 101) drugs and free LPV values were taken from previous TLC-ART 101 study.⁴ AUC_{PBMC}, area under the PBMC drug concentration-time curve extrapolated to infinity; -, not detected; NA, not available.

^aUnpaired t-test, $p < 0.05$ between formulations.

^b $n = 2$.

Table 5

Target Mononuclear Cell Values of Free Drugs for Current ATV, RTV and TFV and Previously Reported Free LPV

Free Drugs	ATV	RTV ^a	TFV ^a	LPV
AUC _{PBMC} (h·μM)	13 ^b	59 (29-86) ^d	260 (197-301) ^d	22 (10-33) ^c
LNMC				
24 h (μM)	0.33 ^b	0.14 (0.01-0.45) ^d	1.81 (0.29-9.3) ^d	-
192 h (μM)	0.03 ^b	-	0.11 ^d	-
LNMC/plasma				
24 h	57 ^b	1.6 ^d	13 ^d	-
LNMC/PBMC				
24 h	11 ^b	0.76 ^d	1.8 ^d	-

Geometric Mean (95% CI).

Free drugs scaled to equivalent DcNP dosages. DcNP containing ATV drugs scaled to equivalent DcNP containing LPV (TLC-ART 101⁴) drug dosages.

DcNP containing LPV (TLC-ART 101) drugs and free LPV values were taken from previous TLC-ART 101 study.⁴

AUC_{PBMC} area under the PBMC drug concentration-time curve extrapolated to infinity.

AUC_{PBMC}, area under the PBMC drug concentration-time curve extrapolated to infinity; -, not detected; NA, not available.

^aRTV and TFV merged with previous free drugs results.⁴

^b
n = 2.

^c
n = 3.

^d
n = 5.

Table 6
 MBPK Model Results of the Current ATV-RTV-TFV DcNP and Comparison With Previously Reported LPV-RTV-TFV TLC-ART 101 MBPK Modeling Results

Model Parameters	Atazanavir-DcNP			Lopinavir-DcNP (TLC-ART 101)		
	ATV	RTV	TFV	LPV	RTV	TFV
k_{21} (1/h)	0.15 (0.1-0.3)	0.40 (0.35-0.46)	0.05 (-)	0.03 (-)	0.24	0.13 (-)
k_{31} (1/h)	0.05 (-)	0.05 (-)	0.1 (-)	0.12	0.19	0.15 (-)
k_{41} (1/h)	0.7 (-)	0.5 (-)	0.15 (-)	0.3	0.02	0.18 (-)
tlag1 (h)	0.25 (-)	0.3 (-)	1	2.2 (1.1-2.9)	2.1 (1-2.9)	0.1 (-)
tlag2 (h)	16 (9-25)	41 (35-46)	23 (-)	11 (8-13)	39 (35-44)	24 (20-29)
tlag3 (h)	440 (336-520)	186 (169-199)	106 (76-132)	262 (250-281)	182 (169-196)	122 (119-125)
V5_DcNP (L/kg)	1259 ^d (569-1680)	67 (22-94)	0.7 (0.5-0.9)	7 ^d (6-8)	10 (7-13)	0.17 (0.15-0.21)
k_{75} (1/h)	0.04 ^d (0.01-0.06)	0.19 (0.06-0.26)	0.026 (0.009-0.03)	0.7 ^d (0.6-0.9)	0.43 (-)	0.020 (0.018-0.03)
k_{76} (1/h)	-	-	1.7 (0.6-2.5)	-	-	1.4 (-)
k_{78} (1/h)	-	-	0.06 (-)	-	-	0.07 (-)
k_{87} (1/h)	-	-	0.02 (-)	-	-	0.03 (-)
V7_Free (L/kg)	113 (97-133)	79 (56-122)	1.1 (0.8-1.3)	84 (82-85)	68 (67-69)	1.7 (1.5-2.1)
K_{07} (1/h)	0.29 (-)	0.08 (0.03-0.12)	0.4 (0.08-2)	0.08 (0.07-0.09)	0.10 (0.08-0.12)	0.58 (0.56-0.62)

Parameters according to schematic depicted in Figure 1.

DcNP containing ATV drugs scaled to equivalent DcNP containing LPV (TLC-ART 101⁴) drug dosages.

DcNP containing LPV (TLC-ART 101) drugs parameters values were taken from previous TLC-ART 101 MBPK study,¹²

k_{21} , rate of DcNP absorption into the first delayed compartment; k_{31} , rate of DcNP absorption into the second delayed compartment; k_{41} , rate of DcNP absorption into the third delayed compartment; tlag1, delayed constant of delayed compartment 1; tlag2, delayed constant of delayed compartment 2; tlag3, delayed constant of delayed compartment 3; V5_DcNP, central compartmental apparent volume for DcNP; V7_Free, central compartmental apparent volume for free drug; k_{75} , rate of degradation of DcNP into free drug between central compartments; k_{76} , rate of absorption of free drug; k_{78} , rate from periphery to central free compartment; k_{87} , rate from central free compartment to periphery; k_{07} , rate of elimination; -, not available or not applicable.

^dUnpaired t-test $p < 0.05$ between formulations